AQUATIC ECOLOGY

REVISTA DE Biología Tropical

https://doi.org/10.15517/rev.biol.trop..v72i1.56835

Iron and Manganese concentrations in leaf tissues of *Rhizophora mangle* (Rhizophoraceae): implications for energetic metabolism

Sávia Soares Pascoalini[1]*; https://orcid.org/0000-0003-3236-8304
Dielle Meire de Santana Lopes[1]; https://orcid.org/0000-0002-9951-0179
Antelmo Ralph Falqueto[2]; https://orcid.org/0000-0003-3146-1873
Verônica D'Addazio[3]; https://orcid.org/0000-0003-4496-9238
Adriano Alves Fernandes[2]; https://orcid.org/0000-0002-5016-0745
Marcelo Barcellos da Rosa[4]; https://orcid.org/0000-0001-5959-0381
Andreia Barcelos Passos Lima Gontijo[2]; https://orcid.org/0000-0003-3422-4398
Mário Luiz Gomes Soares[5]; https://orcid.org/0000-0002-3312-7257
Ivoney Gontijo[2]; https://orcid.org/0000-0002-4251-4689
Edilson Romais Schmildt[2]; https://orcid.org/0000-0002-3457-7997
Helia Del Carmen Farías Espinoza[6]; https://orcid.org/0000-0001-6776-0838
Bryan Brummelhaus de Menezes[4]; https://orcid.org/0000-0002-3431-7669
Lucas Mironuk Frescura[4]; https://orcid.org/0000-0002-7906-0254
Raquel Vidal dos Santos Leopoldo[1]; https://orcid.org/0000-0001-5667-650X
Camila Patricio de Oliveira[1]; https://orcid.org/0000-0002-4211-6752
Lucas de Almeida Leite[2]; https://orcid.org/0009-0009-0960-9019
Neilson Victorino de Brites Júnior[1]; https://orcid.org/0009-0008-8765-9022
Ully Depolo Barcelos[1]; https://orcid.org/0000-0003-4933-5912
Mônica Maria Pereira Tognella[2]; https://orcid.org/0000-0002-1521-8251

1. Espírito-Santo Foundation of Technology (FEST), Federal University of Espírito Santo, Vitória, ES CEP 29075-910, Brazil; savia.pascoalini@gmail.com (*Correspondence), dielle.slopes@gmail.com, vidalquel@gmail.com, patricio.camila@hotmail.com, neilsonbrites@gmail.com, ullydbarcelos@gmail.com
2. Department of Agrarian and Biological Sciences, Federal University of Espírito Santo, São Mateus, ES CEP 29932-900, Brazil; antelmofalqueto@gmail.com, afernandesufes@gmail.com, albarcelos@hotmail.com, ivoneygontijo@yahoo.com.br, e.romais.s@gmail.com, bio.lucasdealmeidaleite@gmail.com, monica.tognella@gmail.com
3. Department of Oceanography and Ecology, Federal University of Espírito Santo, Vitória, ES CEP 29075-910, Brazil; veronicadaddazio@yahoo.com
4. Department of Chemistry, Federal University of Santa Maria, Camobi Campus, Santa Maria, RS CEP 97105-900, Brazil; marcelobdarosa@gmail.com, bryanmenezesqmc@gmail.com, lmironuk15@gmail.com
5. Faculty of Oceanography, Rio de Janeiro State University, Rio de Janeiro, RJ CEP 20550-900, Brazil; mariolgs@gmail.com
6. Center for Technological Sciences of Land and Sea, Vale do Itajaí University, Itajai, SC CEP 88302-901, Brazil; heliafarespinoza@gmail.com

Received 28-IX-2023. Corrected 06-V-2024. Accepted 08-VIII-2024.

ABSTRACT

Introduction: Iron (Fe) and manganese (Mn) are bioessential micronutrients for plants but can impair the energetic metabolism when present at high levels.

Objective: To assess the photosynthetic performance and oxidative damages in *Rhizophora mangle* L. leaf tissues at low and high concentrations of Fe (74 and 195 mg kg^{-1}; Fe_{leaf}) and Mn (65 and 414 mg kg^{-1}; Mn_{leaf}).

Methods: Photosynthetic pigments, chlorophyll *a* fluorescence, leaf CO_2 assimilation and gas exchange and $DPPH^{\bullet}$ radical scavenging capacity were sampled in *R. mangle* growing in estuarine forests in the North region of Espírito Santo State and the extreme South of Bahia State (Brazil) showing low and high Fe_{leaf} and Mn_{leaf}.

Results: Effects of high Fe and Mn were not identified on pigment levels. The increase in Fe_{leaf} and Mn_{leaf} at the levels observed in this assessment had a positive effect on the number of reaction centers and on the efficiency of the oxygen-evolving complex, evaluated as K-band, while no changes were found in the parameters related to the excitation trapping efficiency at the active center of photosystem II. Distinct interference patterns of Fe and Mn on the functional processes of photosynthesis were identified, especially on CO_2 assimilation and reactive oxygen species metabolism, with major effects on CO_2 assimilation and carboxylation efficiency of Rubisco at high Mn_{leaf}.

Conclusion: These findings demonstrate the efficiency of *R. mangle* in positively regulating the electron transport chain in response to high Fe and Mn, at least in terms of the preservation of structure and functionality of the plant photosynthetic apparatus. Moreover, interference of high Mn_{leaf} in *R. mangle* occurs at non-stomatal and biochemical levels. There is an antagonistic interference of these trace elements with the physiology of *R. mangle*, which is a dominant species in Brazilian mangroves.

Key words: JIP-test; CO_2 assimilation; $DPPH^{\bullet}$; photosynthesis; Doce River.

RESUMEN

Concentraciones de hierro y manganeso en tejidos foliares de *Rhizophora mangle* (Rhizophoraceae): implicaciones para el metabolismo energético

Introducción: El hierro (Fe) y el manganeso (Mn) son micronutrientes bioesenciales para las plantas, pero pueden afectar el metabolismo energético cuando están presentes en niveles altos.

Objetivo: Evaluar el desempeño fotosintético y los daños oxidativos en tejidos foliares de *Rhizophora mangle* L. a bajas y altas concentraciones de Fe (74 y 195 mg kg^{-1}; Fe_{leaf}) y Mn (65 y 414 mg kg^{-1}; Mn_{leaf}).

Métodos: Se muestrearon pigmentos fotosintéticos, fluorescencia de clorofila a, asimilación e intercambio de gases de CO_2 foliar y capacidad de eliminación de radicales $DPPH^{\bullet}$ en *R. mangle* que crece en bosques de estuarios en la región Norte del estado de Espírito Santo y el extremo Sur del Estado de Bahía (Brasil) mostrando Fe_{leaf} y Mn_{leaf} bajos y altos.

Resultados: No se identificaron efectos de niveles elevados de Fe y Mn en los niveles de pigmento. El aumento de Fe_{leaf} y Mn_{leaf} en los niveles observados en esta evaluación tuvo un efecto positivo en el número de centros de reacción y en la eficiencia del complejo generador de oxígeno, evaluado como banda K, mientras que no se encontraron cambios en los parámetros relacionados con la eficiencia de atrapamiento de excitación en el centro activo del fotosistema II. Se identificaron distintos patrones de interferencia de Fe y Mn en los procesos funcionales de la fotosíntesis, especialmente en la asimilación de CO_2 y el metabolismo de las especies reactivas de oxígeno, con efectos importantes en la asimilación de CO_2 y la eficiencia de carboxilación de Rubisco a niveles altos de Mn_{leaf}.

Conclusión: Los hallazgos demuestran la eficiencia de *R. mangle* en la regulación positiva de la cadena de transporte de electrones en respuesta a los altos niveles de Fe y Mn, al menos en términos de preservación de la estructura y funcionalidad del aparato fotosintético de la planta. Además, la interferencia de Mn_{leaf} alto en *R. mangle* se presenta a niveles no estomáticos y bioquímicos. Hay interferencia antagónica de estos oligoelementos con la fisiología de *R. mangle*, que es una especie dominante en los manglares brasileños.

Palabras clave: JIP-test; asimilación de CO_2; $DPPH^{\bullet}$; fotosíntesis; Río Doce.

INTRODUCTION

Anthropogenic activities such as petroleum exploration, mining, industrial activities, and other human urban activities are the main sources of trace elements in mangroves (Celis-Hernandez et al, 2020). In Brazil, in 2015, the collapse of the Fundão Dam in Mariana occurred, releasing 40 to 60 million m^3 of mining tailings into the Doce River, the sediment plume, containing trace metals, reached the ocean and coastal region,

potentially affecting mangrove areas (Sá et al., 2021; Tognella et al., 2022). These compounds impose an energy drain on plants; at least in the long-term, persistently high concentrations in mangrove sediments can cause damage to environmental health and affect plant growth, energetic metabolism, and cell structure, thus inducing changes in the ecosystem structure (Wang et al., 2003).

Iron (Fe) and manganese (Mn) are bio-essential micronutrients for plant growth and development for being directly involved in metabolic processes (Najafpour et al., 2014; Taiz et al., 2017; Varma & Jangra, 2021). Both elements have a direct relationship with plant photosynthesis. Fe plays an important role as a component of enzymes that participate in electron transfer (redox reactions), such as cytochromes, being reversibly oxidized and reduced through electron transfer between Fe^{2+} and Fe^{3+}. Besides, chlorophyll (Chl) biosynthesis and maintenance of the structural integrity of photosynthetic reaction centers and light-harvesting compounds (LHC) subunits require Fe. In the photosynthetic electron transport chain (ETC), Fe acts as a cofactor in photosystems II and I (PSII and PSI, respectively) and in the cytochrome (Cyt) b_6/f complex (Taiz et al., 2017). Mn ions (Mn^{2+}), in turn, activate several plant enzymes of the citric acid cycle (Krebs cycle), such as decarboxylases and dehydrogenases. The best-defined function of Mn^{2+} is to constitute the oxygen-evolving complex (OEC) associated with PSII through which oxygen (O_2) is produced from water. The OEC is a manganese-calcium ($Mn_4CaO_5(H_2O)_4$) cluster housed in a protein complex (Najafpour et al., 2014).

Despite being important for electron transfer in chloroplasts, excessive Fe and Mn accumulation in leaf tissues leads to increased cellular toxicity due to reactive oxygen species (ROS) overproduction (Gill & Tuteja, 2010). The chloroplast, more specifically the electron acceptor side of PSI associated with the thylakoid membrane, is the main site of ROS production in plant cells (Gill & Tuteja, 2010). In conditions of superreduction of the ETC as an effect of physiological disorders, part of the electron flow is diverted from ferredoxin to O_2, which is reduced to $O_2^{\bullet -}$ via the Mehler reaction (Taiz et al., 2017). Due to high reactivity and toxicity, ROS cause damage to proteins, lipids, carbohydrates, and DNA, ultimately resulting in cell death (Bailey-Serres & Mittler, 2006). $O_2^{\bullet -}$ ions can donate electrons to Fe^{+3} to generate the reduced form Fe^{+2}, which reduces the H_2O_2 formed by dismutation of $O_2^{\bullet -}$ into $OH^{\bullet}$ (Gill & Tuteja, 2010). In this sense, oxidative stress is triggered by disturbances in the photosynthetic electron flow through the ETC. Under normal conditions, electron flow leads to reduction of $NADP^+$ to NADPH, which is used in the Calvin Cycle to reduce CO_2 to carbohydrates (Taiz et al., 2017). Oxidative stress occurs when ROS generation exceeds the capacity of the plant to maintain cellular redox homeostasis or to scavenge the toxic O_2 molecules (Gill & Tuteja, 2010).

Nevertheless, plants have evolved a sophisticated antioxidant system comprised of specific protective mechanisms to defend themselves against oxidant injury (Gholami et al., 2012). It is well established that the ability to tolerate environmental stress is associated with the expression of an efficient antioxidative system, which provides the first line of defense against the toxic effects of enhanced ROS levels (Gill & Tuteja, 2010). This antioxidative system is composed of antioxidant enzymes as superoxide dismutase (SOD), ascorbate peroxidase (APX), guaiacol peroxidase (GPX), catalase (CAT), monodehydroascorbate reductase (MDHAR), dehydroascorbate reductase (DHAR) and glutathione reductase (GR) as well as nonenzymatic metabolites of low molecular weight like ascorbic acid (Vitamin C), glutathione (GSH), proline (Pro), α-tocopherol (Vitamin E), carotenoids and flavonoids (Mittler et al., 2004).

The antioxidant potential can also be evaluated in plant tissues by assessing the capacity to scavenge the 1,1-Diphenyl-2-picrylhydrazyl free radical ($DPPH^{\bullet}$) (Menezes et al., 2021). The $DPPH^{\bullet}$ assay provides rapid results to evaluate the scavenging efficiency of extracts from *Rhizophora mangle* leaf tissues against ROS,

maintaining the flow of electrons along the ETC as well as CO_2 assimilation at high rates.

This work aims to evaluate the photosynthetic performance and the integrity of the antioxidant defense mechanisms of the true mangrove species *R. mangle* in response to high levels of Fe and Mn in leaf tissues. The present findings contribute to better understand the role of Fe and Mn in carbon assimilation and evidence how beneficial these elements are. Thus, carbon assimilation, Chl *a* fluorescence, photosynthetic pigments, and $DPPH^{\bullet}$ radical scavenging activity were compared in plants from different mangrove areas containing the highest and lowest leaf concentrations of Fe and Mn. Such evaluations allowed to demonstrate how these elements drain energy from plants, and that their persistence in the sediment can induce a long-term loss of environmental health. These approaches are highly relevant in the current century, since coastal eutrophication and the increase in atmospheric carbon have been widely discussed (Gilman et al., 2008; Sanders et al., 2014). Our experiment was conducted in several mangrove systems in the states of Espírito Santo and Bahia, Brazil, following the failure of the Fundão tailings dam in 2015 (Instituto Brasileiro do Meio Ambiente e dos Recursos Naturais Renováveis [IBAMA], 2019).

MATERIALS AND METHODS

Study area, plant material, and sampling: The sampling locations are shown in Fig. 1 and further described in Tognella et al. (2022). The areas were selected according to the concentrations of Fe and Mn in leaf tissues (hereafter, "Fe_{leaf}" and "Mn_{leaf}", respectively) of *R. mangle*, which is the dominant species in the studied plots. Thus, four estuaries (Aracruz, Barra Nova, São Mateus and Caravelas, within the geographic coordinates (19°93'97"-17°72'70" S & 40°21'32"-39°28'32" W) showing low and high Fe_{leaf} and Mn_{leaf} were selected in fringe and basin forests in the North region of Espírito Santo State and the extreme South of Bahia State (Brazil).

Five plants were randomly selected and marked in each plot. Sampling and measurements were performed in fully expanded but not visibly senescent leaves of the second pair of the branch from the apex. Measurements were made in the morning (between 8:00 and 12:00). Plant height varied from 0.68 to 1.64 m and 0.88 to 1.54 m at the low and high Fe_{leaf} sites, respectively. All sites were inserted within predefined areas (fixed plots). The sampling locations showed statistical similarities regarding the minimum and maximum values of salinity (3.7-33.4 psu and 3.7-29.6 psu at the low and high Fe and Mn sites, respectively). Mean annual rainfall ranges between 1 100 and 1 400 mm at the study sites (Alvarez et al., 2014; Instituto Nacional de Meteorologia, 2019). In addition, precipitation and relative air humidity in the source areas ranged from 115.76 to 119.17 mm and 75.5 to 87.0 %, respectively between April and August 2019 (Instituto Nacional de Meteorologia, 2019), characterized as dry period. Sampling was conducted at low tide.

Sediment and leaf sampling: Sediment samples were collected in the intertidal area using collectors built with a 50 cm PVC pipe. The material was obtained in two depths of 0 to 5 cm (surface) and 5 to 15 cm. In each plot, simple samples were randomly collected (for each depth) and homogenized to remove roots, shell fragments, leaves and branches and thus form a composite sample for each depth. Next, the sediment samples were placed into previously identified plastic bags, kept in a cool box with ice and taken to the laboratory for freezer storage.

To quantify the concentration of metals in leaf tissues of *R. mangle*, healthy mature leaves showing no signs of herbivory were sourced from five trees in each location, stored in paper bags and maintained under refrigeration until processing. In the laboratory, leaves were dried at 60 °C until constant weight was attained.

Sediment and leaf chemical analysis: Analysis of metals in sediments was performed according to the United States Environmental

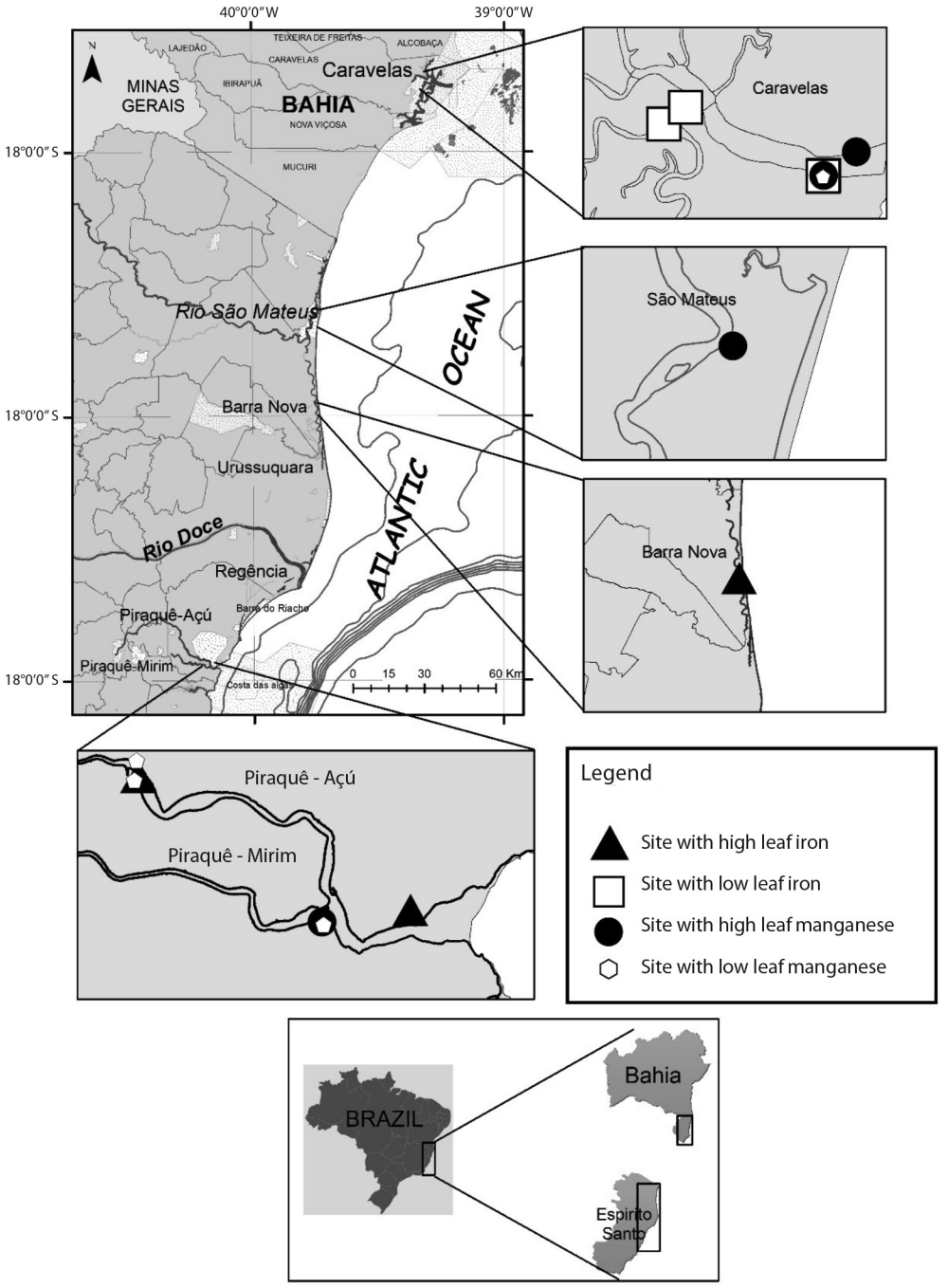

Fig. 1. Location of the sampling sites in Northern Espírito Santo and Southern Bahia. Triangle, square, circle and hexagon identify the sites with high and low leaf Fe concentration and high and low leaf Mn concentration, respectively.

Protection Agency (USEPA) Method 3051A (USEPA, 2013). Dry and homogenized sediment (about 0.5 g) was digested with HNO_3:HCl (3:1; 12 ml) in Teflon tubes in a microwave oven (CEM, Marx X-Press) using the following program: 1st ramp 25-175 °C in 5:30 min; and 2nd ramp 25-175 °C in 4:30 min (both with a power setting of 1 600 W). Afterwards, the solution was cooled, filtered through a Whatman n° 1 filter, diluted to 100 ml in a volumetric flask and analyzed by ICP-MS (Inductively Coupled Plasma Mass Spectrometry; Agilent, CX7 500).

The plant material was dried, ground and submitted to nitroperchloric digestion. Fe_{leaf} and Mn_{leaf} were subsequently quantified by atomic absorption spectrophotometry (Silva, 2009).

Pigment quantification: Leaf samples of 5 g (fresh mass) were frozen at -30 °C and ground in liquid nitrogen with a mortar and pestle to form a fine powder, which was transferred to test tubes and homogenized in 15 ml of 90 % acetone solutions and 0.5 g l^{-1} of calcium carbonate ($CaCO_3$). Next, the test tubes were immediately stored at 2 °C for 24 h for complete pigment extraction (modified by Arar, 1997). The samples were then filtered, and the supernatant was collected and stored in amber flasks at -30 °C pending analysis by spectrophotometry. The extraction procedure was carried out at room temperature in dark conditions to minimize Chl degradation by enzymatic action. Ice cold extraction solvents were used. The extraction time was kept to a minimum to reduce degradation of the analyzed pigments.

Subsequently, the optical density readings were determined on a spectrophotometer (Genesys 10S UV-Vis, Thermo Fisher Scientific, Waltham, USA) at 470, 645 and 663 nm. Determination of photosynthetic pigment concentrations was performed according to the equations proposed by Wellburn (1994): chlorophyll a (Chla) a = (12.25 x A_{663} – 2.79 x A_{645}), chlorophyll b (Chlb) = (21.5 x A_{645} – 5.1 x A_{663}), and carotenoids (Car) = (1 000 x A_{470} – 1.82 x Chla – 85.02 Chlb/198); values were expressed in mg ml^{-1} of fresh mass, where A_{470}, A_{645} and A_{663} represent the absorbance at 470, 645 and 663 nm, respectively.

Chlorophyll *a* fluorescence and leaf gas exchange: Chl *a* fluorescence was measured at room temperature using a plant efficiency analyzer (*Handy-PEA, Hanstech Instruments Ltd.*, King's Lynn, Norkfolk, UK), as in Strasser & Govindjee (1992). Previously, leaves were adapted to the dark during 30 min using leaf clips (*Hansatech Instruments Ltd.*). Fluorescence rise OJIP trace was induced by 1 s pulses of red light (650 nm, 3 000 µmol (photon) m^{-2} s^{-1}). O and P refer to the initial and maximum fluorescence intensity considered here at 50 µs (F_0) and 300 ms, respectively. J (≅ 2 to 3 ms) and I (≅ 30 ms) are inflection points between O and P levels. The fluorescence transients OJIP curves were analyzed according to the JIP-test (Strasser et al., 2004). L and K-bands were calculated as $V_{OK} = (F_{100\mu s} - F_0)/(F_{300\mu s} - F_0)$ and V_{OJ} $[(F_{300\mu s} - F_0)/(F_{2ms} - F_0)]$ (Srivastava & Strasser 1997; Strasser & Stirbet, 2001). A detailed description of parameters and their meaning can be found elsewhere (Strasser et al., 2004) and briefly addressed in Table 1.

Leaf CO_2 assimilation (*A* [µmol m^{-2} s^{-1}]), stomatal conductance (*gs* [mol m^{-2} s^{-1}]), intercellular CO_2 concentration (*Ci* [µmol m^{-2} s^{-1}]) and leaf transpiration rate (*E* [mmol m^{-2} s^{-1}]) were estimated in the same leaves used to measure Chl *a* fluorescence; for that, portable infrared gas analyzers (models *Lci,* L*ci T* and L*cpro T*, ADC, *BioScientific Ltd.*, Hoddesdon, England) were used. The gas chamber was maintained at ambient conditions, the average photon flux density in the chamber was 200 ± 28.7 and 316 ± 46.9 µmol m^{-2} s^{-1}, with the average leaf temperature reaching 29.5 ± 0.4 and 31.0 ± 0.5 °C for the Fe and Mn treatments, respectively. Estimation of water-use efficiency was calculated and determined as intrinsic water-use efficiency (WUE_{int} = *A*/*gs* [µmol (CO_2) mol^{-1}(H_2O)]) and instantaneous water-use efficiency (WUE_{ins} = *A*/*E* [µmol (CO_2) $mmol^{-1}$(H_2O)]) (Krauss, et al, 2006). *A* and *Ci* were used to estimate the carboxylation efficiency

Table 1
Abbreviations of the JIP-test parameters, formulas, and description of the data derived from the transient of Chl *a* fluorescence.

Fluorescence Parameters	Description
F_t	Fluorescence at time t after onset of actinic illumination
$F_o \cong F_{20ms}$	Minimal fluorescence, 11cep all PSII RCs are open
$F_K \cong F_{0.3ms}$	Fluorescence intensity at the K-step (0.3 ms) of OJIP
$F_J \cong F_{2ms}$	Fluorescence intensity at the J-step (2 ms) of OJIP
$F_I \cong F_{30ms}$	Fluorescence intensity at the I-step (30 ms) of OJIP
F_P (=F_m)	Maximal fluorescence at the peak P, 11cep all PSII RCs are closed
$F_v \cong F_m - F_0$	Maximal 11ceptor11 fluorescence
Area	Total complementary 11cep between the fluorescence induction curve and F_0 and F_m
$V_J = (F_J - F_0)/(F_m - F_0)$	Relative 11ceptor11 fluorescence at the J-step
L-band = $V_{OK} = (F_t - F_0)/(F_K - F_0)$	Variable fluorescence between steps O (50 μs) and K (300 μs), indicative of the energetic connectivity between the subunits associated with PSII
K-band = $V_{OJ} = (F_t - F_0)/(F_J - F_0)$	Variable fluorescence between steps O (50 μs) and J (2 ms), which is an indicative of stability of oxygen 11ceptor11n complex (OEC)
$ABS/RC = M_0.(1/V_J).(1/ \varphi P_0)$	Absorption flux per active reaction center (RC) at t = 0.
$TR_0/RC = M_0.(1/V_J)$	Trapped energy flux per RC (at t = 0)
$ET_0/RC = M_0.(1/V_J).\psi_{E0}$	Electron transport flux per RC (at t = 0)
$DI_0/RC = [(ABS/RC) - (TR_0/RC)]$	Dissipated energy flux per RC at t = 0.
$RC/CS_0 = \varphi P_0.(V_J/M_0).(ABS/CS)$	Total number of active reaction center per cross section
$\varphi P_0 = TR_0/ABS = [1 - (F_0/F_m)] = F_v/F_m$	Maximum quantum yield of primary photochemistry at t = 0).
$\varphi D_0 = 1 - \varphi P_0 = (F_0/F_m)$	Quantum yield of energy dissipation (at t = 0).
$\varphi E_0 = (1 - F_0/F_m)\ (1 - V_J)$	Quantum yield for PSII electron transport (ET)
$\delta R_0 = (1 - V_I)/(1 - V_J)$	Quantum yield for reduction of the end electron acceptors at the PSI 11ceptor side
$PI_{ABS} = RC/ABS.\varphi P_0/(1 - \varphi P_0).\psi_{E0}/(1 - \psi_{E0})$	Performance index based on absorption
$PI_{Total} = PI(ABS) \times [\delta R_0/(1 - \delta R_0)]$	Performance index (potential) for energy conservation from photons absorbed by PSII to the reduction of PSI end acceptors

of ribulose-1,5-bisphosphate-carboxylase/oxygenase (Rubisco) (*A*/Ci) (Zhang et al., 2001).

DPPH• radical scavenging assay: The free radical scavenging ability of the extracts was determined using the DPPH• method (Dal Prá et al., 2013; Huang et al., 2005). To obtain the extracts, which were referred to as working solutions (WS), plant samples were dried in an oven and then diluted in methanol (two, five, ten or twenty times). The tests were carried out by adding aliquots of 15, 25 and 35 μL of each WS into cuvettes containing 3.0 mL of DPPH methanolic solution (0.2 mmol l^{-1}), which were kept protected from light for 60 min. Tests were made in triplicate. Measurements were performed on a Perkin Elmer Lambda 16 spectrophotometer, monitoring the absorbance of the samples at 517 nm. The blank consisted of 3.0 ml of methanol containing 15, 25 or 35 μl of the respective WS. A solution containing DPPH served as negative control. The percentage of DPPH• scavenging was calculated as [1 – (As – Ab)/ (Ac – Ab)] x 100, where As, Ab and Ac are the absorbance of samples, blank and negative control, respectively.

The IC_{50} values (concentration necessary to inhibit 50 % of the DPPH• radical) were determined by means of linear regression. As analyses were performed in triplicate, the mean and the standard deviation were used to represent the IC_{50} of each sample.

Statistical analysis: Data were submitted to normality (Shapiro-Wilk) and homogeneity (Barttlet) tests. To determine differences between the physiological parameters in relation to the concentration of Fe and Mn (low x high), the non-normal data were analyzed via the non-parametric Mann-Whitney U test, while normally distributed data were assessed through the t-student test. In the basic statistical analyses, Excel or the statistical treatment package Statistica (STATSOFT®) were used. The significant threshold was set at 0.05 for all tests.

RESULTS

Fe and Mn concentration: In *R. mangle*, the low and high Fe_{leaf} were 74 and 195 mg kg^{-1}, while the low and high Mn_{leaf} were 65 and 414 mg kg^{-1}, respectively. The concentration of Mn in the sediment was 101 and 239 mg kg^{-1} at the sites with the lowest and highest concentrations, respectively, while no variation in Fe concentration was observed among the sites (≅ 22 252 mg kg^{-1}) (Fig. 2).

Pigment quantification: There was no significant difference in the concentrations of Chla, Chlb and Car in the leaves of *R. mangle* growing in both high and low Fe and Mn sites (Table 2).

Chl *a* fluorescence: The OJIP transients of samples exposed to high and low Fe_{leaf} and Mn_{leaf} showed a typical polyphasic rise with the fluorescence signal rising from the initial fluorescence level (F_0) to the maximal fluorescence level (Fm), with well-defined intermediate J and I steps (Fig. 3). High Fe_{leaf} increased the fluorescence yield (F_0 and Fm) and the area beneath the fluorescence curve between F_0 and Fm (Table 3). In contrast, high Fe did not affect quantum yield for primary photochemistry, for electron transport and for energy dissipation, φP_0, φE_0, and φD_0, respectively. The

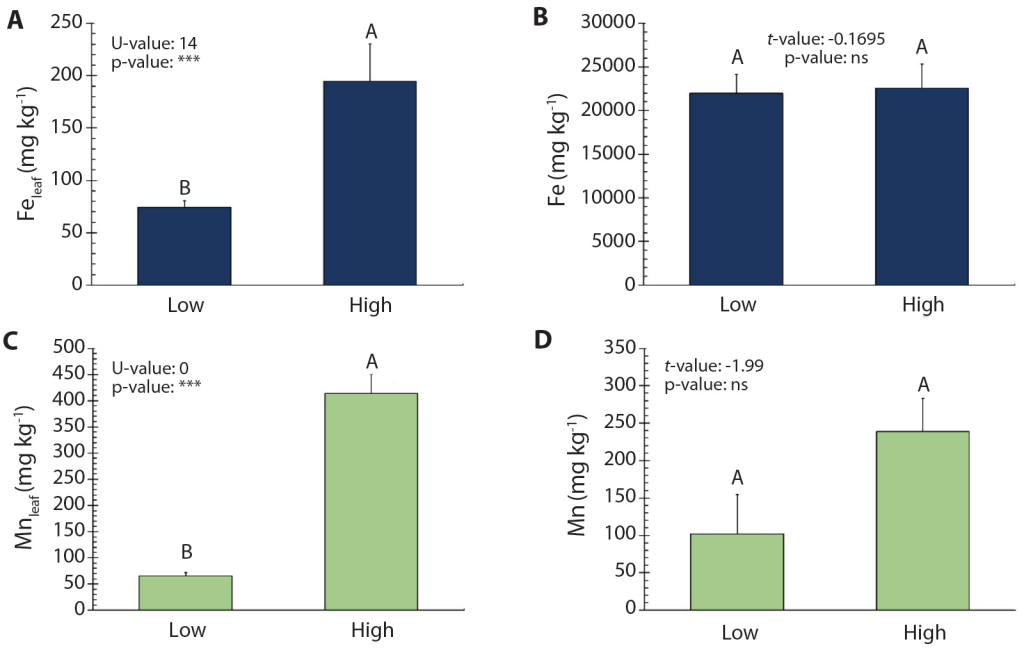

Fig. 2. Concentration (mean ± SE) of Fe and leaves (**A**) and sediments (**B**); Mn in leaves (**C**) and in sediments (**D**) of the *Rhizophora mangle*, referring to sampling sites (Low and High concentration). Different letters indicate significant difference between sites ($P < 0.05$; n.s.: non-significative; ^{U} or ^{t}: Mann-Whitney U test or *t*-student, respectively).

Table 2

Concentration of pigments (mean ± SE) in *Rhizophora mangle*, referring to sampling sites (low and high concentration of Fe and Mn in the leaf) in Northern Espírito Santo and Southern Bahia.

	Fe_{leaf}				Mn_{leaf}			
	Low	High	U or *t* value	P-value	Low	High	U or *t* value	P-value
Chla (μg mL^{-1})	297.65 ± 23.21 ^{A}	238.94 ± 139. 00 ^{A}	12.00 ^{U}	n.s.	249.20 ± 31.77 ^{A}	331.09 ± 62.58 ^{A}	50.00 ^{U}	n.s.
Chlb (μg mL^{-1})	212.75 ± 16.70 ^{A}	147.21 ± 76.90 ^{A}	-1.36 ^{t}	n.s.	165.74 ± 19.22 ^{A}	231.59 ± 43.25 ^{A}	46.00 ^{U}	n.s.
Car (μg mL^{-1})	589.64 ± 58.78 ^{A}	576.89 ± 189.00 ^{A}	-0.08 ^{t}	n.s.	597.92 ± 72.67 ^{A}	628.86 ± 68.39 ^{A}	-0.31 ^{t}	n.s.

Chla (chlorophyll a- μg ml^{-1}), Chlb (chlorophyll b- μg ml^{-1}), Car (carotenoids- μg ml^{-1}). Different letters indicate significant differences between sites ($P < 0.05$; n.s.: non-significative; ^{U} or ^{t}: Mann-Whitney U test or *t*-student, respectively).

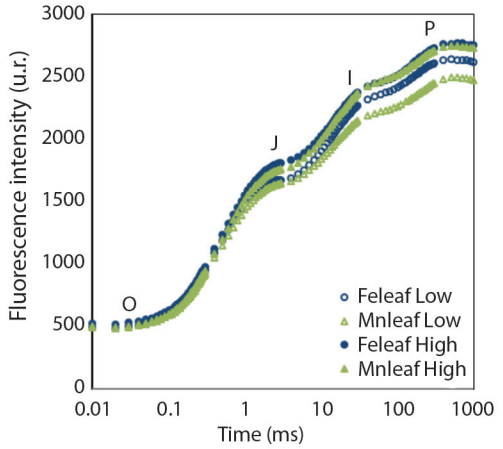

Fig. 3. The OJIP chlorophyll a fluorescence transient curve in *Rhizophora mangle*, referring to sampling sites (low and high concentration of Fe and Mn in the leaf).

specific energy fluxes per reaction center (RC) for absorption (ABS/RC), trapping (TR_0/RC) and electron transport (ET_0/RC) were lower at high Fe without variation in the specific energy flux for dissipation (DI_0/RC). Furthermore, the total number of active reaction centers per cross section (RC/CS_0) and the quantum yield for reduction of the end electron acceptors at the PSI acceptor side (δR_0) increased about 15.3 % and 4.51 % at high Fe, and the performance indexes (PI_{ABS} and PI_{Total}) were statistically similar among sites, with average values of 20.92 and 13.19, respectively. Moreover, the increase in Fe_{leaf} increased the energetic connectivity between the subunits associated with PSII and the stability of OEC, which can be visualized by lower values of L and K-bands, respectively, while no changes were registered in the oxidoreduction capacity of Q_A by electrons originated from P680 (V_J or J-step values) among sites (Table 3).

The increase in Mn_{leaf} did not affect the basal fluorescence yield (F_0) in *R. mangle*, but increased Fm and Area. Contrastingly, *R. mangle* high in Mn_{leaf} showed enhanced values of quantum yield for photochemistry and electron transport (φP_0 and φE_0, respectively), and decreases the quantum yield of energy dissipation (φD_0) at high Mn_{leaf}. A greater number of active reaction centers was recorded at high Mn_{leaf}, the absorption (ABS/RC) and dissipation (DI_0/RC) energy flux were lower, although the capture (TR_0/RC) and electron transport flux (further than Q_A^-) or ET_0/RC did not vary. As for the performance indexes (PI_{ABS} and PI_{Total}), only PI_{ABS} showed a statistically significant difference among sites, with higher values (23.33) being detected at the sites where Mn_{leaf} was higher. The opposite occurred with the the quantum yield for reduction of the end electron acceptors at the PSI acceptor side (δR_0), and L-band at high Mn_{leaf}. No changes were seen in the K-band or V_J (Table 3).

Leaf gas exchange: Leaf CO_2 assimilation and gas-exchange variables were analyzed to better characterize the effects of Fe_{leaf} and Mn_{leaf} on *R. mangle* photosynthetic performance (Fig. 4). The present results indicate that photosynthesis was differently influenced by Fe and Mn in leaf tissue. *E, gs, A*, and CE (carboxylation efficiency = *A/Ci*) values increased in leaf tissue of *R. mangle* containing high Fe, while *Ci*

Table 3

Mean values (± SE) of the parameters calculated from the JIP-test obtained from *Rhizophora mangle* plants in the sampling of Fe and Mn (low and high concentration of Fe and Mn in the leaf) sites in Northern Espírito Santo and Southern Bahia.

Parameters	Fe_{leaf}					Mn_{leaf}				
	Low	High	Percentage of change in reduction	U or *t* value	P-value	Low	High	Percentage of change in reduction	U or *t* value	P-value
Area	65 073.51 ± 1 305.51 ^{B}	71 012.28 ± 1573.50 ^{A}	--	2.92 ^{t}	**	66 382.32 ± 1136.52 ^{A}	67 127.65 ± 1257.73 ^{A}	n. s.	1 759.00 ^{U}	n. s.
F_0	434.37 ± 4.41 ^{B}	474.93 ± 3.65 ^{A}	--	444.00 ^{U}	***	438.10 ± 4.15 ^{A}	447.01 ± 4.22 ^{A}	n. s.	1.50 ^{t}	n. s.
F_m	2 644.97 ± 26.51 ^{B}	2 768.17 ± 31.95 ^{A}	--	2.98 ^{t}	**	2 497.76 ± 29.73 ^{B}	2 751.91 ± 40.58 ^{A}	---	4.64 ^{U}	***
ϕP_0	0.802 ± 0.001 ^{A}	0.798 ± 0.006 ^{A}	n. s.	-1.56 ^{t}	n. s.	0.792 ± 0.002 ^{B}	0.806 ± 0.001 ^{A}	---	830.00 ^{U}	***
ϕE_0	0.377 ± 0.004 ^{A}	0.361 ± 0.006 ^{A}	n. s.	1 123.00 ^{U}	n. s.	0.357 ± 0.007 ^{B}	0.374 ± 0.005 ^{A}	---	2.04 ^{t}	*
ϕD_0	0.197 ± 0.002 ^{A}	0.202 ± 0.002 ^{A}	n. s.	1.50 ^{t}	n. s.	0.207 ± 0.002 ^{A}	0.193 ± 0.001 ^{B}	6.76 %	832.00 ^{U}	***
J-Step	0.459 ± 0.005 ^{A}	0.441 ± 0.008 ^{A}	n. s.	1 257.5 ^{U}	n. s.	0.435 ± 0.008 ^{A}	0.454 ± 0.006 ^{A}	n. s.	1.79 ^{t}	n. s.
ABS/RC	1.89 ± 0.037 ^{A}	1.75 ± 0.034 ^{B}	7.40 %	-2.68 ^{t}	**	1.85 ± 0.037 ^{A}	1.74 ± 0.038 ^{B}	5.94 %	-2.11 ^{t}	*
TR_0/RC	1.51 ± 0.026 ^{A}	1.39 ± 0.025 ^{B}	7.94 %	-3.06 ^{t}	**	1.46 ± 0.026 ^{A}	1.40 ± 0.030 ^{A}	n. s.	1 559.00 ^{U}	n. s.
ET_0/RC	0.704 ± 0.011 ^{A}	0.629 ± 0.014 ^{B}	10.65 %	688.00 ^{U}	***	0.654 ± 0.016 ^{A}	0.642 ± 0.012 ^{A}	n. s.	1 728.00 ^{U}	n. s.
DI_0/RC	0.382 ± 0.011 ^{A}	0.356 ± 0.009 ^{A}	n. s.	1 138.00 ^{U}	n. s.	0.390 ± 0.011 ^{A}	0.340 ± 0.009 ^{B}	12.82 %	1 150.00 ^{U}	***
RC/CS_0	279.12 ± 3.81 ^{B}	321.85 ± 5.26 ^{A}	---	6.74 ^{t}	***	284.89 ± 5.69 ^{B}	310.68 ± 5.69 ^{A}	---	1 156.00 ^{U}	***
PI_{ABS}	21.43 ± 0.871 ^{A}	20.41 ± 0.989 ^{A}	n. s.	0.77 ^{t}	n. s.	19.37 ± 1.00 ^{B}	23.33 ± 1.04 ^{A}	---	1 255.00 ^{U}	**
PI_{Total}	13.02 ± 0.628 ^{A}	13.36 ± 0.652 ^{A}	n. s.	1 224.00 ^{U}	n. s.	12.42 ± 0.621 ^{A}	13.86 ± 0.661 ^{A}	n. s.	1 476.00 ^{U}	n. s.
δR_0	0.377 ± 0.004 ^{B}	0.394 ± 0.005 ^{A}	---	2.55 ^{t}	*	0.396 ± 0.005 ^{A}	0.372 ± 0.004 ^{B}	6.06 %	1 137.00 ^{U}	***
L-Band	0.167 ± 0.001 ^{A}	0.164 ± 0.001 ^{B}	1.79 %	-2.37 ^{t}	*	0.171 ± 0.001 ^{A}	0.165 ± 0.0008 ^{B}	3.50 %	1 354.00 ^{U}	*
K-Band	0.365 ± 0.006 ^{A}	0.340 ± 0.006 ^{B}	6.84 %	-3.20 ^{t}	**	0.367 ± 0.001 ^{A}	0.348 ± 0.007 ^{A}	n. s.	-1.82 ^{t}	n. s.

Different letters indicate significant differences between sites ($P < 0.05$; n.s.: non-significative; ^{U} or ^{t}: Mann-Whitney U test or *t*-student, respectively). Parameters expressed in relative units.

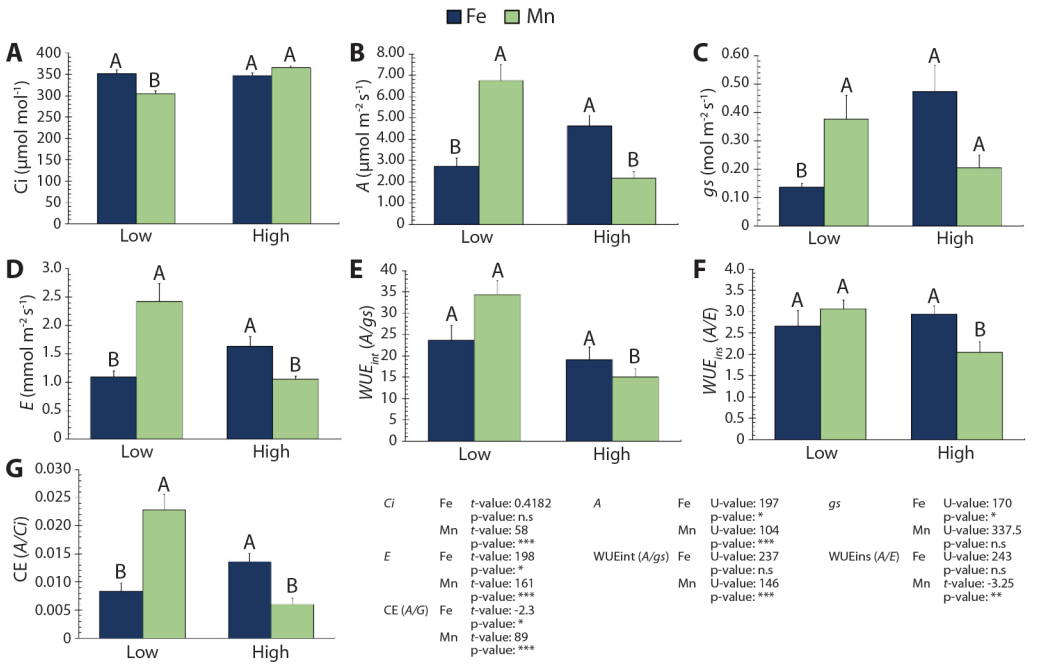

Fig. 4. Gas exchange parameters (mean ± SE) in *Rhizophora mangle*, referring to sampling sites (Low and High concentration of Fe and Mn in the leaf). **A.** *Ci* (intercellular CO_2 concentration), **B.** *A* (net carbon assimilation rate), **C.** *gs* (stomatal conductance), **D.** *E* (transpiration rate), **E.** WUE_{int} (intrinsic water use efficiency - *A/gs*), **F.** WUE_{ins} (instantaneous water use efficiency) and **G.** *CE* (carboxylation efficiency). Different letters indicate significant differences between sites ($P < 0.05$; n.s.: non-significative; ^{U} or ^{t}: Mann-Whitney U test or *t*-student, respectively).

and WUE_{int} (intrinsic water use efficiency = *A/gs*) and WUE_{ins} (instantaneous water use efficiency = *A/E*) remained unchanged. Conversely, despite exhibiting better photochemical performance, the rise in Mn_{leaf} increased *Ci* and decreased *E, A,* WUE_{int}, WUE_{ins} and CE (Fig. 4).

DPPH• radical scavenging assay: Higher Fe_{leaf} in *R. mangle* reduced the concentration of the extract needed to scavenge DPPH• by 50 % (IC_{50}). For Mn_{leaf}, however, the opposite effect was observed (Fig. 5).

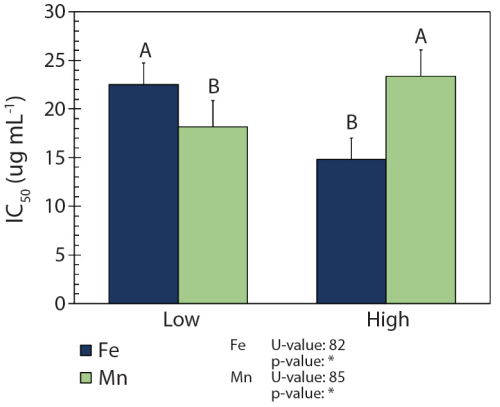

Fig. 5. Antiradical activity IC_{50} against DPPH• (mean ± SE) in *Rhizophora mangle*, referring to sampling sites (Low and High concentration of Fe and Mn in the leaf). Different letters indicate significant differences between sites ($P < 0.05$; ^{U}: Mann-Whitney U test).

DISCUSSION

The effects triggered by Fe and Mn exposure were seen in all evaluated parameters and resulted in physiological changes in *R. mangle*. We understand that, although iron and manganese concentrations in leaf tissues have a great influence on photosynthetic processes, other factors also act as regulators.

Nevertheless, we observed alterations occurred among locations where Fe_{leaf} and Mn_{leaf} were significantly different, and involved analyses of photosynthetic pigments, transient Chl *a* fluorescence, gas exchange, CO_2 assimilation, oxidative stress, and the detoxification capacity of plants, evaluated here as DPPH• radical scavenging activity. The achieved results will certainly allow to understand the successful strategies of the *R. mangle* tree to cope with the altered environment as well as its capacity to cleanse sediment and water.

The difference in Fe uptake and accumulation allowed us to select the study areas. Such differences in absorption, given the invariability of the element in the sediment, may be associated with the presence of other trace elements at higher concentrations, *e.g.* Mn, (data not shown), as observed in the sediment of the site showing lower Fe_{leaf} (data not shown). Conversely, low Mn sediment concentration was found under high Fe_{leaf} (data not shown). The content of clay and soil organic matter also influences the availability of Fe to plants, since there is a tendency to retain Fe in muddy soils. Adequate levels of organic matter improve Fe uptake due to its acidifying and reducing properties; moreover, certain humic substances could form chelates under adverse pH conditions (Dechen & Nachtigall, 2006). Besides, Fe absorption decreases with increased concentrations of Ca, Mg, Cu, Zn and especially Mn (Jones-Junior, 2012). High concentrations of Mn in acidic soils can competitively inhibit Fe absorption (Malavolta, 1980). Such Mn values are independent of the results observed in this study, considering the different sampling sites. Like Fe, Mn in the sediment tends to form stable and insoluble compounds, suitable for the adsorption of other metals (Förstner & Witmann, 1981). However, upon contact with mangrove sediments, imported particulate manganese is reduced, due to the physical-chemical characteristics of this compartment. This process makes the element soluble, facilitating its export to adjacent environments in the form of Mn (II) (Vidal & Becker, 2006). Therefore, it is possible that the variation in Mn concentration in the sediment observed in this study is associated with areas of export (low concentrations) and import (high concentrations).

Chl *a* fluorescence transient in *R. mangle* under low and high Fe_{leaf} and Mn_{leaf} revealed the three typical OJIP phases (O-J, J-I and I-P), indicating that all samples remained photosynthetically active (Strasser & Stirbet, 2001) independently of metal concentration. The increase in F_0 and Fm at the sites with higher Fe_{leaf} resulted in higher area above the fluorescence curve (Area) between F_0 and Fm. As stated by Joliot and Joliot (2002), the area represents the electron acceptor pool sizes of PSII, including Q_A and Q_B. In this investigation, the area over the fluorescence curve was slightly but significantly ($P \leq 0.05$) increased by 9.12 % under high Fe_{leaf} compared to low Fe_{leaf}, showing that the elevation in Fe_{leaf} improves the electron transfer rates at the donor side of PSII and increases Q_A pool size (Gao et al., 2022; Mehta et al., 2010). Furthermore, despite the increase in Fm at high Mn_{leaf}, there were no changes in F_0 or Area. It has been suggested that high Fm occurs when thylakoid membranes are preserved, thus leading to the clustering of light-harvesting complexes (LHCII) associated with PSII (Schreiber & Neubauer, 1987).

The levels of F_0 were only increased by about 2.03 % ($P \geq 0.05$) at high Mn_{leaf}, while at high Fe_{leaf} they were 9.3 % ($P \leq 0.05$) higher than at low Fe_{leaf}. Nonetheless, although F_0 values showed a significant rise under high Fe_{leaf}, no alterations were registered in parameters related to efficiency, as similarly observed at high Mn_{leaf}. F_0 is associated with the donor side of PSII, with the adjustment capacity of antenna pigment level or with the excitation trapping efficiency at the active center of PSII. In this regard, the current findings indicate that the increased F_0 values observed at high Fe_{leaf} are demonstrated at antenna pigment level, as verified by decreased levels of Chlb, since the values of L and K-bands were reduced and the parameters related to the excitation trapping efficiency at the active center of PSII (φP_0, φE_0, φR_0, TR_0/RC, PI_{ABS} and PI_{Total}) remained

unchanged. K-band and L-band are associated with the donation of electrons from the OEC to PSII and with the connection/disconnection (or energetic connectivity) of the PSII core antenna (LHC), respectively (Strasser et al., 2004). The observed decreases/invariability of K-band and L-band values evidence that concentrations of Fe and Mn, as those registered in leaf tissues of *R. mangle* grown under *in situ* conditions, exert some protective effect on electron donor and acceptor sides of PSII, thus maintaining the integrity of the OEC and LHC. It is worth noting that the OEC uses Mn as an essential cofactor in the oxidation of water (Strasser et al., 2004); moreover, as well as the ferredoxin protein, the end electron acceptor of PSI contains Fe in its molecular structure.

Analysis of the efficiency of the energy flow per reaction center (RC) revealed reduction in absorption (ABS/RC), trapping (TR_0/RC) and transport (ET_0/RC) and no change in dissipation (DI_0/RC) in plants growing under high Fe_{leaf}. Similar results were obtained for *R. mangle* from sites with high Mn_{leaf}; there were significant decreases in DI_0/RC and ABS/RC and no alterations in TR_0/RC or ET_0/RC. The energy flow parameters per RC are calculated as the total number of photons absorbed, captured, transported, and dissipated from all RCs divided by the total number of active RCs (Mehta et al., 2010). Thus, the ratio of active/inactive RCs influences the values of energy fluxes. Consequently, as disclosed herein, reductions in all energy fluxes occur when the number of RCs is improved; increases in RC/CS_0 of 15.3 % ($P \leq 0.05$) and 9.05 % ($P < 0.05$) were found in *R. mangle* grown under high Fe_{leaf} and Mn_{leaf}, respectively. Increased RC/CS_0 in *R. mangle* can reduce the effects of photoinhibition and thus result in lower energy dissipation. These statements are reinforced by the decreases seen in ABS/RC values, which indicate that both metals increased the antenna size of active RCs; such observations were more important in *R. mangle* growing under high Fe_{leaf} and Mn_{leaf} conditions.

Collectively, these results indicate the efficiency of the photosynthetic apparatus, since the excitation energy was absorbed and captured by the Chl molecules and directed towards electron transport to reduce pheophytin, Q_A and the other electron acceptors in the ETC (Taiz et al., 2017). The increase in Fm and the reduction and/or invariability of parameters connected to energy dissipation mechanisms, as DI_0/RC and φD_0, are thus explained. In general, although it is widely accepted that PSII is extremely susceptible to several types of environmental stresses, the observed increases in *R. mangle* Fe_{leaf} and Mn_{leaf} have a positive regulatory effect, at least in terms of preservation of structure and functionality of the plant photosynthetic apparatus. Mechanisms of photosynthetic regulation related to the ability to dissipate excitation energy leading to photoprotection have been suggested and discussed (Wang et al., 2016). Carotenoids participate in the photoprotection system, and the invariability of this pigment is consistent with the results found for the increase in Fe_{leaf} and Mn_{leaf} (Szabó et al., 2005).

For a deeper understanding of the role of Fe and Mn as elements in carbon assimilation in *R. mangle*, a detailed gas-exchange analysis was carried out associated with oxidative stress and antiradical activity. It is generally agreed that environmental alterations directly affect carbon assimilation in plants, considering that photosynthesis is highly vulnerable to metal toxicity (Ahmad et al., 2008; Barcelos et al., 2022); the effects are multi-dimensional and influence photosynthetic CO_2 fixation under controlled conditions as well as *in situ*. The current results evidenced distinct interference patterns of Fe and Mn with the functional processes of photosynthesis, including the antioxidant capacity of *R. mangle*, despite the improved performance of the ETC of chloroplast.

Unlike the results obtained at high Mn_{leaf}, the antioxidant system of *R. mangle,* evaluated here through the free radical scavenging activity, undoubtedly functioned as a protection system under high Fe_{leaf}. As a result, high CO_2 assimilation capacity and carboxylation efficiency (CE) of ribulose-1.5-bisphosphate carboxylase oxygenase (Rubisco) were maintained. Thus, increased *Ci* as well as decreased

CO_2 assimilation, WUE_{int}, WUE_{ins} and CE under excessive Mn are linked to oxidative damage buildup in *R. mangle* leaf tissue, despite its plasticity in light energy utilization. These are alarming results, since such estuarine systems undergo great climatic variability (Lopes et al., 2019; Pascoalini et al., 2022). Additionally, the high nutrient content intensifies plant vulnerability to drought, especially under low atmospheric humidity and/or limited freshwater input, thus compromising the use of water by the vegetation (Lovelock et al., 2009; Oliveira et al., 2022).

The increases in *A* and *gs* under high Fe_{leaf} conditions, which were associated with the invariability of *Ci*, suggest that the enhanced CO_2 flux into *R. mangle* leaves caused by stomatal opening was a relevant factor for the increase in *A*. In contrast, the lower *A, gs* and *E* values at high Mn_{leaf}, which were associated with higher *Ci* levels, imply that *R. mangle* photosynthesis was limited by non-stomatal factors, besides indicating that Mn interfered with stomatal regulation. Reductions in CO_2 assimilation is likely to be associated not only with lower CO_2 entry into leaves, but also some biochemical limitation in CO_2 fixation within the chloroplasts, which is related to lower Rubisco activity and changes in the capacity for ribulose-1,5-bisphosphate regeneration (Alves et al., 2011; Wang et al., 2022). Investigations about the role of Mn on photosynthesis have evidenced repression of specific genes, particularly of those nuclear-encoded small subunits of Rubisco (Sheen, 1994). Consequently, Rubisco content and CO_2 assimilation are reduced. According to Li et al. (2010), the regulatory role of Mn-excess appears to be linked with the accumulation of soluble sugars, as sucrose, glucose, and fructose, but it remains to be further clarified. The authors also report that the reduced CO_2 assimilation in Mn-excess leaves was not accompanied by Chl, since there were no differences in the contents of Chla or Chlb between the tested Mn treatments. Such finding is consistent with the unchanged concentrations of photosynthetic pigments described here for *R. mangle* under high Mn_{leaf} conditions.

Globally, mangroves play a particularly important role in maintaining biodiversity hotspots. However, despite the environmental and economic values attributed to mangroves, these ecosystems are constantly prone to anthropogenic or natural actions that result in increased heavy metal concentrations in sediments, which often act as sinks for these toxic elements. Our results showed that Fe and Mn affected the physiological performance of *R. mangle* in a different manner. Nevertheless, when taking all physiological parameters into consideration, we verified that the effects of high Fe_{leaf} at antenna pigment level did not impair the carbon gain of *R. mangle* trees at the evaluated sites, since K-band values were reduced and there were no changes in parameters related to the excitation trapping efficiency at the active center of PSII. Rises in Fe_{leaf} and Mn_{leaf} in *R. mangle* at the levels recorded in this evaluation increased RC/CS_0, thus suggesting a positive regulatory effect at least in terms of preservation of structure and functionality of the plant photosynthetic apparatus. This study also identified distinct interference patterns of Fe and Mn with the functional processes of photosynthesis, especially with CO_2 assimilation and ROS metabolism. The most pronounced effects were observed in CO_2 assimilation and carboxylation efficiency of Rubisco at high Mn_{leaf}. Thus, interference of high Mn_{leaf} in *R. mangle* occurs at non-stomatal and biochemical levels. Further research should be conducted under controlled conditions and including higher doses of the metals to expand our understanding of the regulatory role of excessive Fe and Mn on the metabolism of *R. mangle* at the whole-tree level. The current findings may aid in predicting alterations resulting from the effects of environmental changes, which make the mangrove forest even more vulnerable.

This assessment described the antagonism between Fe and Mn regarding the physiology of *R. mangle*, which is a dominant species in Brazilian mangroves. Moreover, attention is drawn to the coastal eutrophication processes currently taking place in the global mangrove

area. *R. mangle* appears to be participating in bioremediation, but the physiological responses disclosed herein raise concern about the interference of long-term eutrophication in ecosystem productivity.

Ethical statement: the authors declare that they all agree with this publication and made significant contributions; that there is no conflict of interest of any kind; and that we followed all pertinent ethical and legal procedures and requirements. All financial sources are fully and clearly stated in the acknowledgments section. A signed document has been filed in the journal archives. Funding: This research was financially supported by Renova Foundation via its Technical-Scientific Cooperation Agreement nº 30/2018 with Espírito Santo Foundation of Technology (FEST). Declaration of Competing Interest: The authors declare no conflict of interest.

ACKNOWLEDGMENTS

This research was developed under the Aquatic Biodiversity Monitoring Program, Environmental Area I, established by the Technical-Scientific Cooperation Agreement nº 30/2018 between Espírito Santo Foundation of Technology (FEST) and Renova Foundation, published in Brazil's Official Gazette (Diário Oficial da União). The authors would like to thank the CAPES/FAPES Cooperation—Postgraduate Development Program—PDPG and the Laboratory of Environmental Geochemistry and the Laboratory of Geological Oceanography of the University of Espírito Santo for their analyses of metals and sediment.

REFERENCES

Ahmad, M. S. A., Hussain, M., Ijaz, S., & Alvi, A. K. (2008). Photosynthetic performance of two mung bean (*Vigna radiata* L. Wilczek) cultivars under lead and copper application. *International Journal of Agriculture & Biology, 10*(2), 167–176.

Alvares, C. A., Stape, J. L., Sentelhas, P. C., Gonçalves, J. L. M., & Sparovek, G. (2014). Köppen´s climate classification map for Brazil. *Meteorologische Zeitschrift, 22*(6), 711–728.

Alves, A. A., Guimarães, L. M. S., Chaves, A. R. M., DaMatta, F. M., & Alfenas, A. C. (2011). Leaf gas exchange and chlorophyll a fluorescence of Eucalyptus urophylla in response to *Puccinia psidii* infection. *Acta Physiology Plantarum, 33*, 1831–1839.

Arar, E. J. (1997). *Method 447.0-Determination of chlorophylls a and b and identification of other pigments of interest in marine and freshwater algae using high performance liquid chromatography with visible wavelength detection*. U.S. Environmental Protection Agency, Washington.

Bailey-Serres, J., & Mittler, R. (2006). The roles of reactive oxygen species in plant cells. *Plant Physiology, 141*(2), 311.

Barcelos, U. D, Gontijo, A. B. P. L., Fernandes, A. A., Falqueto, A. R., Pascoalini, S. S., Lopes, D. M. S., Schmildt, E. R., Leite, S., & Tognella, M. M. P. (2022). The role of iron on the growth and development of the seedlings of *Rhizophora mangle* L. *Scientific Research and Essays, 17*(3), 35–45.

Celis-Hernandez, O., Giron-Garcia, M. P., Ontiveros-Cuadras, J. F., Canales-Delgadillo, J. C., Perez-Ceballos, R. Y., Ward, R. D., Acevedo-Gonzales, O., Armstrong-Altrinm, J. S., & Merino-Ibarra, M. (2020). Environmental risk of trace elements in mangrove ecosystems: an assessment of natural vs oil and urban inputs. *Science Total Environment, 730*, 138643.

Dal Prá, V., Dolwitsch, C. B., & Da Silveira, G. D. (2013). Supercritical CO_2 extraction, chemical characterization and antioxidant potential of *Brassica oleracea* var. capitata against $HO^{\bullet}$, $O_2^{\bullet-}$ and ROO. *Food Chemistry, 141*(4), 3954–3959.

Dechen, A. R., & Nachtigall, G. R. (2006). Micronutrientes. In M. S. Fernandes (Ed.), *Nutrição Mineral de Plantas* (pp. 327–354). SBCS: Viçosa.

Förstner, U., & Witmann, G. T. W. (1981). Metal pollution in the aquatic environment (2nd Ed.). Springer-Verlag: New York.

Gao, D., Ran, C., Zhang, Y., Wang, X., Lu, S., Geng, Y., Guo, L., & Shao, X. (2022). Effect of different concentrations of foliar iron fertilizer on chlorophyll fluorescence characteristics of iron-deficient rice seedlings under saline sodic conditions. *Plant Physiology and Biochemistry, 185*, 112-122.

Gholami, M., Rahemi, M., Kholdebarin, B., & Rastegar, S. (2012). Biochemical responses in leaves of four fig cultivars subjected to water stress and recovery. *Scientia Horticulturae, 148*, 109–117.

Gill, S. S., & Tuteja, N. (2010). Reactive oxygen species and antioxidant machinery in abiotic stress tolerance in

crop plants. *Plant Physiology and Biochemistry, 48*(12), 909–930.

Gilman, E. L., Ellison, J., Duke, N. C., & Field, C. (2008). Threats to mangroves from climate change and adaptation options: A review. *Aquatic Botany, 89*(2), 237–250.

Huang, D., Ou, B., & Prior, R. L. (2005). The chemistry behind antioxidant capacity assays. *Journal of Agricultural and Food Chemistry, 53*(6), 1841–1856.

Instituto Brasileiro de Meio Ambiente e Recursos Naturais Renováveis. (2019). *Laudo Técnico Preliminar: Impactos ambientais decorrentes do desastre envolvendo o rompimento da Barragem de Fundão, em Mariana, Minas Gerais* (Downloaded: April 24, 2021). http://www.ibama.gov.br/phocadownload/barragemdefundao/laudos/laudo_tecnico_preliminar_Ibama.pdf

Instituto Nacional de Meteorologia. (2019). *Mapa de Estações Meteorológicas.* https://mapas.inmet.gov.br/

Joliot, P., & Joliot, A. (2002). Cyclic electron transfer in plant leaf. *Proceedings of the National Academy of Sciences, 99*(15), 10209–10214.

Jones-Junior, B. J. (2012). *Plant nutrition and soil fertility manual* (2nd Ed.). CRC Press; Boca Raton.

Krauss, K. W., Twilley, R. R., Doyle, T. W., & Gardiner, E. S. (2006). Leaf gas exchange characteristics of three neotropical mangrove species in response to varying hydroperiod. *Tree Physiology, 26*, 959–968.

Li, Q., Chen, L. S., & Jiang, H. X. (2010). Effects of manganese-excess on CO_2 assimilation, ribulose-1,5-bisphosphate carboxylase/oxygenase, carbohydrates and photosynthetic electron transport of leaves, and antioxidant systems of leaves and roots in *Citrus grandis* seedlings. *BMC Plant Biology, 10*, 42.

Lopes, D. M. S., Tognella, M. M. P., Falqueto, A. R., & Soares, M. L. G. (2019). Salinity variation effects on photosynthetic responses of the mangrove species *Rhizophora mangle* L. growing in natural habitats. *Photosynthetica, 57*(4), 1142–1155.

Lovelock, C. E., Ball, M. C., Martin, K. C., & C. Feller, I. (2009). Nutrient enrichment increases mortality of mangroves. *PloS One, 4*(5), e5600.

Malavolta, E. A. (1980). *Elementos de nutrição mineral de plantas*. Ceres: São Paulo.

Mehta, P., Jajoo, A., Mathur, S., & Bharti, S. (2010). Chlorophyll a fluorescence study revealing effects of high salt stress on photosystem II in wheat leaves. *Plant Physiology And Biochemistry, 48*(1), 16–20.

Menezes, B. B., Frescura, L. M., Duarte, R., Villetti, M. A., & Rosa, M. B. (2021). A critical examination of the DPPH method: Mistakes and inconsistencies in stoichiometry and IC50 determination by UV Vis spectroscopy. *Analytica Chimica Acta, 1157*, 338398.

Mittler, R., Vanderauwera, S. M., & Van Breusegem, F. (2004). Reactive oxygen gene network of plants. *Trends in Plant Science, 9*(10), 490–498.

Najafpour, M. M., Isaloo, M. A., Eaton-Rye, J. J., Tomo, T., Nishihara, H., Satoh, K., Carpentier, R., Shen, J. R., & Allakhverdiev, S. I. (2014). Water exchange in manganese-based water-oxidizing catalysts in photosynthetic systems: From the water-oxidizing complex in photosystem II to nano-sized manganese oxides. *BBA Bioenergetics, 1837*(9), 1395–1410.

Oliveira, G. C., Broetto, S. G., Pereira, O. J., Penha, J. S., Lopes, N. G. M., & Silva, D. M. (2022). Effects of different levels of metal exposure and precipitation regimes on chlorophyll a fluorescence parameters in a coastal Brazilian restinga species. *Journal of Photochemistry and Photobiology, 12*, 100153.

Pascoalini, S. P., Tognella, M. M. P., Falqueto, A. R., & Soares, M. L. G. (2022). Photosynthetic efficiency of young *Rhizophora mangle* L. in a mangrove in southeastern Brazil. *Photosynthetica, 60*(3), 337–349.

Sá, F., Longhini, C. M., Costa, E. S., Silva, C. A., Cagnin, R. C., Gomes, L. E. O., Lima, A. T., Bernardino, A. F., & Neto, R. R. (2021). Time-sequence development of metal(loid)s following the 2015 dam failure in the Doce river estuary, Brazil. *Science of The Total Environment, 769*, 144532.

Sanders, C. J., Eyre, B. D., Santos, I. R., Machado, W., Luiz-Silva, W., Smoak, J. M., Breithaupt, J. L., Ketterer, M. E., Sanders, L., Marotta, H., & Silva-Filho, E. (2014). Elevated rates of organic carbon, nitrogen, and phosphorus accumulation in a highly impacted mangrove wetland. *Geophysical Research Letters, 41*, 2475–2480.

Schreiber, U., & Neubauer, C. (1987). The polyphasic rise of chlorophyll fluorescence upon onset of strong continuous illumination. II. Partial control by the photosystem II donor side and possible ways of interpretation. *Zeitschrift für Naturforschung C, 42*, 1246–1254.

Sheen, J. (1994). Feedback control of gene expression. *Photosynthesis Research, 39*(3), 427–438.

Silva, F. C. (2009). *Manual de análises químicas de solos, plantas e fertilizantes* (2nd Ed.). Embrapa Informação Tecnológica: Brasília.

Srivastava, A., & Strasser, R. J. (1997). Constructive and destructive actions of light on the photosynthetic apparatus. J*ournal of Scientific & Industrial Research, 56*(9), 133–148.

Strasser, R. J, & Govindjee. (1992). The Fo and O-J-I-P fluorescence rise in higher plants and algae. In J. H. Argyroudi-Akoyunoglou (Ed.), *Regulation of Chloroplast Biogenesis* (pp. 423–426). Springer: New York.

Strasser, R. J, & Stirbet, A. D. (2001). Estimation of the energetic connectivity of PS II centres in plants using the fluorescence rise O-J-I-P. *Mathematics and Computers in Simulation, 56*(4), 451–461.

Strasser, R. J., Tsimilli-Michael, M., & Srivastava, A. (2004). Analysis of the chlorophyll a fluorescence transient. In G. Papageorgiou & Govindjee (Eds.), *Advances in photosynthesis and respiration chlorophyll a fluorescence: a signature of photosynthesis* (pp. 321–362). Springer: Dordrecht.

Szabó, I., Bergantino, E., & Giacometti, G. M. (2005). Light and oxygenic photosynthesis: energy dissipation as a protection mechanism against photo-oxidation. *EMBO reports*, *6*(7), 639–634.

Taiz, L., Zeiger, E., Møller, I.M., & Murphy, A. (2017). *Fisiologia e desenvolvimento vegetal* (6th Ed.). Artmed: Porto Alegre.

Tognella, M. M. P., Falqueto, A. R., Espinoza, H. D. C. F., Gontijo, I., Gontijo, A. B. P. L., Fernandes, A. A., Schmildt, E. R., Soares, M. L. G., Chaves, F. O., Schmidt, A. J., Lopes, D. M. S., Barcelos, U. D., D'Addazio, V., Lima, K. O. O., Pascoalini, S. S., Paris, J. O., Brites-Júnior, N. V., Porto, L. A., Almeida-Filho, E., ... Albino, J. (2022). Mangroves as traps for environmental damage to metals: The case study of the Fundão Dam. *Scince of the Total Environment, 806*(4), 150452.

United States Environmental Protection Agency (2013). *Electronic Code of Federal Regulations, Title 40-Protection of Environment, Part 423–Steam Electric Power Generating Point Source Category. Appendix A to Part 423–126: Priority Pollutants.* https://www.law.cornell.edu/cfr/text/40/appendix-A_to_part_423

Varma, S., & Jangra, M. (2021). Heavy metals stress and defense strategies in plants: An overview. *Journal of Pharmacognosy and Phytochemistry, 10*(1), 608–614.

Vidal, R. M. B., & Becker, H. (2006). Distribuição de manganês, ferro, matéria orgânica e fosfato nos sedimentos do manguezal do Rio Piranji, Ceará. *Arquivo de Ciências do Mar*, *39*(1), 34–43.

Wang, D., Hu, P., & Tie, N. (2022). Responses of photosynthesis and antioxidant activities in *Koelreuteria paniculata* young plants exposed to manganese stress. *South African Jounal of Botany, 147*, 340–348.

Wang, Q. R., Cui, Y. S., Liu, X. M., Dong, Y. T., & Christie, P. (2003). Soil contamination and uptake of heavy metals at polluted sites in China. *Journal of Environmental Scince Health, 38*(5), 823–838.

Wang, Y., Qu, T., Zhao, X., Tang, X., Xiao, H., & Tang, X. (2016). A comparative study of the photosynthetic capacity in two green tide macroalgae using chlorophyll fluorescence. *SpringerPlus, 5*, 775.

Wellburn, A. R. (1994). The spectral determination of chlorophylls a and b, as well as total carotenoids, using various solvents with spectrophotometers of different resolution. *Journal of Plant Physiology, 144*(3), 307–313.

Zhang, S., Li, Q., Ma, K., & Chen, L. (2001). Temperature-dependent gas exchange and stomatal/non-stomatal limitation to CO_2 assimilation of *Quercus liaotungensis* under midday high irradiance. *Photosynthetica, 39*, 383–388.